Phys Chem Minerals (2000) 27: 332–341

ORIGINAL PAPER

N.H. de Leeuw · S.C. Parker · C.R.A. Catlow · G.D. Price

Modelling the effect of water on the surface structure and stability of forsterite

Received: 4 August 1999 / Revised, accepted: 11 October 1999

Abstract We describe the application of atomistic simulation techniques to investigate the effect of associative and dissociative adsorption of water on the structures and stabilities of the low-index surfaces of forsterite. All surfaces are amenable to associative adsorption of water, while dissociative adsorption is energetically favourable on all but the non-dipolar {1 0 0} surface. Often, otherwise unstable (dipolar) surfaces are stabilised to a large extent by hydration, e.g. the dipolar {0 1 0} surface. However, on thermodynamic grounds we do not expect associatively adsorbed water to dissociate on all surfaces, as the energies released for dissociative adsorption of water on the non-dipolar {0 1 0} and {1 0 0} surfaces are less than those released for associative adsorption. As such, there is no energetic incentive for the associatively adsorbed water molecules to dissociate. The stabilities of the two terminations of the {0 1 0} surface, the main cleavage plane of forsterite, are reversed when hydroxylated, indicating that some dissolution of the magnesium ions may occur upon hydration, which is shown to be an exothermic process for both surface terminations. The equilibrium morphology was calculated as a way of assessing the change in surface energies. The experimental morphology of forsterite is adequately reproduced, suggesting that the relative stabilities of the surfaces, both unhydrated and hydroxylated, are calculated correctly.

N.H. de Leeuw (✉) · S.C. Parker
School of Chemistry, University of Bath,
Claverton Down, Bath BA2 7AY, UK
e-mail: n.h.deleeuw@bath.ac.uk
e-mail: s.c.parker@bath.ac.uk

C.R.A. Catlow
Davy Faraday Research Laboratory,
Royal Institution of Great Britain,
21 Albemarle Street, London W1X 4BS, UK

G.D. Price
Department of Geological Sciences,
University College London,
Gower Street, London WC1E 6BT, UK

Key words Forsterite · Atomistic simulation · Adsorption of water · Surface reactivity · Morphology

Introduction

Olivine is a common rock-forming mineral which exists as a complete isomorphous series, with compositions ranging from forsterite (Mg_2SiO_4) to fayalite (Fe_2SiO_4). The more common olivines are richer in magnesium than in iron (Dana 1941). Forsterite, the magnesium end member of the olivine group of minerals, consists of SiO_4 tetrahedra linked by magnesium cations in octahedral coordination. It can be synthesized by solid-state reactions between MgO and SiO_2 at elevated temperatures (1100–1400 °C) (Mitchell et al. 1998) and from stoichiometric mixtures in the presence of water at low temperature (500 °C). The presence of water also has a profound effect on the melting point (1890 °C), which increases with pressure under anhydrous conditions but decreases with pressure under water-saturated conditions. For example, at a pressure of 30 kbar the melting point of the anhydrous form has increased to approximately 2030 °C, while the melting point of forsterite under water-saturated conditions at the same pressure has decreased to 1400 °C (Deer et al. 1992).

Because of their prominence as mantle minerals, forsterite and olivine in general have been the subject of much research, both experimental and theoretical. The emphasis of many investigations has naturally been on the mineral's behaviour at high pressures and temperatures, e.g. the determination of high-pressure and high-temperature thermodynamic data (Dubrovinskaya et al. 1997) and the transition mechanism of olivine to high-pressure polymorphs (Kerschhofer et al. 1996). Other recent investigations have included trace element partitioning (Purton et al. 1996, 1997) and grain boundary melting (Hirth and Kohlstedt 1995; Kohlstedt and Zimmerman 1996).

Another important topic is the occurrence and significance of water in forsterite. For example, Kohn

(1996) used H-1 MAS NMR spectroscopy to study dissolved water concentrations in forsterite and found evidence of static water molecules in the form of OH clusters possibly sited at grain boundaries together with OH groups associated with point defects. Wieland et al. (1988) studied forsteritic olivine amongst other minerals in his study on surface-controlled dissolution rates involving activated complexes at the hydrated surfaces. Wright and Catlow (1994) also studied forsterite olivine but used computational methods to calculate the energetics of incorporating water into the bulk crystal. In view of the importance of water in the chemistry of forsterite and its occurrence at grain boundaries, we were interested in investigating both associative and dissociative adsorption of water on the surfaces of forsterite, with a view to assessing its effect on the surface structure and stability. A detailed study of the problem is reported in this paper based on well-established modelling techniques.

Theoretical methods

The surface geometries and energies were modelled using atomistic simulation techniques. These are based on the Born model of solids (Born and Huang 1954) which assumes that the ions in the crystal interact via long-range electrostatic forces and short-range forces, including both the repulsions and the van der Waals attractions between neighbouring electron charge clouds. The long-range Coulombic interactions are calculated using the Parry technique (Parry 1975, 1976) (which is adapted from the well-known Ewald method to 2D periodic systems), whereas the short-range forces are described by parameterised analytical expressions. The electronic polarisability of the ions is included via the shell model of Dick and Overhauser (1958) in which each polarisable ion, in our case the oxygen ion, is represented by a core and a massless shell, connected by a spring. The polarisability of the model ion is then determined by the spring constant and the charges of the core and shell. These are usually obtained by fitting to experimental dielectric constants, when available. In addition, it is often necessary to include angle-dependent forces to allow for partially covalent bonds, for instance in the silica groups and in the water molecules.

We have recently modelled forsterite surfaces using the potential model for SiO_2 derived empirically by Sanders et al. (1984), which was successfully used in many previous studies, to investigate the effect of hydration on the surface structure of quartz (de Leeuw et al. 1999a), in combination with the potential model for MgO derived by Lewis and Catlow (1985) which we used previously in a number of applications, both static calculations (de Leeuw et al. 1995, 1996) and molecular dynamics simulations (de Leeuw and Parker 1998). The resulting potential model has been used successfully in earlier simulations of bulk properties of forsterite, e.g. Price et al. (1987) and Parker and Price (1989); a review of these earlier studies is given by Catlow and Price (1990). The potential parameters for the hydroxide ion using partial charges were those modified from the potential model of Saul et al. (1985) by Baram and Parker (1996), to include a polarisable oxygen ion. They then successfully applied these parameters in their work on hydroxide formation at quartz and zeolite surfaces. The potential model for the intra- and intermolecular water interactions was employed in our investigations of water adsorption on α-alumina surfaces (de Leeuw and Parker 1999b) and its derivation and further application are fully described in a previous paper of molecular dynamics simulations of hydrated MgO surfaces (de Leeuw and Parker 1998a). Although the potentials used are spherically symmetric, inclusion of the shell model means that the water molecule, as represented by four flexible centres consisting of an oxygen core and shell and two hydrogens, is deformable, and the shell model gives a crude representation of the electronic polarisability. The model reproduces many experimental features including coordination and hydrogen-bonding distances and adsorption energies. The potential parameters describing the interactions between water molecules and forsterite surfaces were those successfully used for quartz (de Leeuw et al. 1999) and MgO (de Leeuw et al. 1996) and were obtained, following the approach of Schroder et al. (1992), by modifying the short-range Buckingham potentials, which is necessary because of the fractional charges of the water molecule's oxygen and hydrogen ions. The potential parameters used in this work are collected in Table 1.

Atomistic simulation techniques are appropriate for these calculations because they are capable of modelling systems consisting of a large number of ions (approximately 1800 species per unit cell). By treating a large portion of crystal, we can be confident that the calculated energies are independent of crystal size. We employed energy minimisation techniques to investigate the interactions between the lattice ions and a full monolayer of adsorbed species to identify the strength of interaction with specific surface features. The energy minimisation code employed was METADISE (Watson et al. 1996), which is designed to model dislocations, interfaces and surfaces. Following the approach of Tasker (1979), the crystal consists of a series of charged planes parallel to the surface and periodic in two dimensions. Tasker (1979) identified three different types of surfaces, (1) an uncharged plane with cations and anions in stoichiometric ratio, (2) a stack of charged planes where the repeat unit perpendicular to the surface has no dipole moment, and finally (3) a stack of charged planes where the repeat unit has a dipole moment perpendicular to the surface. In the last instance, the surface needs to be reconstructed to remove the dipole. This is often achieved by creating vacancies in the surface. The crystal is divided into two blocks each comprising two regions, region I and region II, which are periodic in two dimensions lateral to the surface. Region I contains those atoms near the extended defect, in this case the surface layer or solid/water interface, and a few layers immediately below (approximately 180 species per unit cell), and these atoms are allowed to relax to their mechanical equilibrium. Region II contains those atoms further away which represent the rest of the crystal and are kept fixed at their bulk equilibrium position. The energies of the blocks are essentially the sum of the energies of interaction between all atoms. It is necessary to include region II to ensure that the total interaction energy of an ion at the bottom of region I is modelled correctly. The bulk of the crystal is simulated by the two blocks together while the surface is represented by a single block with the top of region I as the free surface. Interfaces such as stacking faults and grain boundaries can be studied by fitting two surface blocks together in different orientations. Both regions I and II need to be sufficiently large for the energy to converge.

The surface energy is a measure of the thermodynamic stability of the surface with a low, positive value indicating a stable surface. The surface energy is given by:

$$\gamma = \frac{U_s - U_b}{A} \quad , \tag{1}$$

where U_s is the energy of the surface block of the crystal, U_b is the energy of an equal number of atoms of the bulk crystal and A is the surface area. For the hydrated surfaces the surface energies were calculated with respect to liquid water in order to assess the stability of the surface in an aqueous environment:

$$\gamma = \frac{U_d - (U_b + U_{H_2O})}{A} \quad , \tag{2}$$

where U_d is the energy of the surface block, suitably hydrated, while U_b is again the energy of the same number of bulk ions and U_{H_2O} is the energy of bulk water. The latter is the sum of the self-energy of water due to the intramolecular forces, and the energy of condensation due to the intermolecular forces. For associative adsorption we calculated the self-energy to be -878.0 kJ mol^{-1} and we obtained the energy of condensation of -43.0 kJ mol^{-1} from molecular dynamics simulations (de Leeuw and Parker 1998a), which agrees well with the experimental value of -43.4 kJ mol^{-1}

Table 1 Potential parameters used in this study. Note: all two-body short range potentials cut off at distances beyond 10 Å and are between oxygen shells where applicable

Charges (e)			Core-shell interaction (eV Å^{-2})
Ions	Core	Shell	
Mg	+2.00000		
Si	+4.00000		
H	+0.40000		
Oxide oxygen (O_{OX})	+0.84819	−2.84819	74.92
Hydroxide oxygen (O_{OH})	+0.90000	−2.30000	74.92
Water oxygen (O_{H_2O})	+1.25000	−2.05000	209.45
Buckingham potential	A (eV)	ρ (Å)	C (eV Å^6)
Mg-O_{OX}	1428.5	0.29453	0
Mg-O_{OH}	941.5	0.29453	0
Mg-O_{H_2O}	490.0	0.29453	0
Si-O_{OX}	1283.9	0.32052	10.66
Si-O_{OH}	983.6	0.32052	10.66
Si-O_{H_2O}	562.0	0.32052	10.66
O_{OX}-O_{OX}	22764.3	0.14900	27.88
O_{OX}-O_{OH}	22764.3	0.14900	13.94
O_{OX}-O_{H_2O}	22764.3	0.14900	28.92
O_{OH}-O_{OH}	22764.3	0.14900	6.97
O_{OH}-O_{H_2O}	22764.3	0.14900	17.14
H-O_{OX}	396.3	0.25000	0
H-O_{OH}	312.0	0.25000	0
H-O_{H_2O}	396.3	0.25000	10.0
Lennard-Jones potential	A (eV Å^{12})		B (eV Å^6)
O_{H_2O} - O_{H_2O}	39344.98		42.15
Morse potential	D (eV)	α (Å^{-1})	r_0 (Å)
H-O_{OH}	7.052500	3.17490	0.94285
H-O_{H_2O}	6.203713	2.22003	0.92376
Three-body potential	k (eV rad^{-2})		Θ_0
H-O_{H_2O}-H	4.2		108.69
O_{OX}-Si-O_{OX}	2.1		109.47
O_{OH}-Si-O_{OH}	2.1		109.47
O_{OX}-Si-O_{OH}	2.1		109.47
Coulombic subtraction		(%)	
H-O_{H_2O} (shell)		50	
H-H		50	
H-O_{OH} (shell)		100	

(Duan et al. 1995). Thus, the new surface energy is simply equivalent to the sum of the energy required to cleave the crystal and then add water to the surface. We need to be confident that in each case the most stable configuration of the surface with adsorbed water layer is found, locating as far as possible the global rather than a local minimum. Thus, many possible configurations were investigated, varying both adsorption sites and the initial position of the water molecule. An alternative approach which is particularly suitable for very complex surfaces including both extended and point defects, (see for example de Leeuw et al. (1999b) on calcium carbonate surfaces) is to use molecular dynamics simulations to move the water over the energy surface. However, these dynamics simulations were not used in the present study. All energies quoted are those of the most stable relaxed surface configurations found.

The calculation of the surface and adsorption energies of dissociative adsorption of water required a value for the energy of dissociation of a water molecule:

$$H_2O_{(g)} + O^{2-}_{(g)} \rightarrow 2(OH)^-_{(g)} \quad . \tag{3}$$

However, this requires the second electron affinity of oxygen, which is material-dependent (Harding and Pyper 1995). This can be overcome by using experimental heats of formation for the reaction:

$$Mg_2SiO_{4(s)} + 4H_2O_{(g)} \rightarrow Si(OH)_{4(g)} + 2Mg(OH)_{2(s)} \quad . \tag{4}$$

The reaction enthalpy for reaction (4) was found to be −151.7 kJ mol^{-1} (Greenberg 1957; Iler 1979; Weast and Astle 1981) and using that, with the calculated lattice energies given in Table 2, the energy of dissociation in reaction (3) was calculated to be −784.4 kJ mol^{-1}. This value then becomes the effective self-energy

Table 2 Calculated lattice energies, where the lattice energy is the energy released when ions at infinity are brought together into the lattice

Lattice energies/kJ mol^{-1}	
$MgO_{(s)}$	−3984.8
$Mg(OH)_{2(s)}$	−3378.3
$SiO_{2(s)}$ (quartz)	−12414.0
$Si(OH)_{4(g)}$	−10784.6

of water, U_{H_2O}, and can be used directly in Eq. (2) when dissociative adsorption is modelled.

Unlike the surface energies, which are calculated with respect to liquid water, we also report the adsorption energies, which are calculated with respect to gaseous water to facilitate direct comparison with energies obtainable by experimental techniques such as temperature-programmed desorption and microcalorimetric measurements.

Results and discussion

Forsterite has an orthorhombic structure with space group Pbnm (Deer et al. 1992). We used the unit cell of $a = 4.7560$ Å, $b = 10.2070$ Å and $c = 5.9800$ Å, $\alpha = \beta = \gamma = 90°$ (Smyth and Hazen 1973), which relaxed to a minimum-energy configuration with $a = 4.7898$, $b = 10.2464$ Å and $c = 5.9863$ Å, $\alpha = \beta = \gamma = 90°$, i.e. very close to the experimental values. The calculated elastic constants are compared with the experimental values (Iishi 1978) in Table 3 and show adequate agreement. The bulk crystal was then cut to obtain the relevant surfaces in a way which kept the SiO_4 units intact, and hence all silicon atoms remain four-coordinated. Previous calculations (Davies 1992) have shown that breaking up the SiO_4 units leads to less stable surfaces and therefore, in this our first study of hydrated forsterite surfaces, we have concentrated on the surfaces where Mg-O bonds rather than Si-O bonds are broken.

We modelled the dissociative and associative adsorption of water at a range of forsterite surfaces which were hydrated up to full monolayer coverage. The reason we model one monolayer of water in static calculations is threefold. Firstly, the results, for example the hydration energies, are directly comparable to most surface science techniques, including temperature-programmed desorption (TPD), which mainly use materials generated under ultrahigh vacuum conditions dosed with gaseous water. Secondly, in static calculations more than one monolayer of water would be modelling the mineral/ice interface rather than liquid water, giving interfacial rather than surface energies and properties. Thirdly, molecular dynamics simulations of MgO in liquid water showed that there is a distinct difference in structure and density between the adsorbed monolayer and the bulk water, and the static calculations with one adsorbed monolayer mimic these MD simulations (de Leeuw and Parker 1998).

For associative adsorption we found that a maximum of one water molecule per 10 Å^2 could be accommodated before a second water layer started to form, which agreed with previous molecular dynamics simulations of MgO in liquid water (de Leeuw and Parker 1998). In that study and also previous simulations of the hydration of calcite and α-alumina surfaces (de Leeuw and Parker 1997; de Leeuw and Parker 1998b, 1999b) we found that water molecules often adsorb flat onto the surface, in agreement with experimental findings of hydrated neutral clay surfaces (Chang et al. 1995). In addition, it is reasonable to expect to find one water molecule per 10 Å^2 if we consider the experimental non-bonded hydrogen-oxygen distance in ice to be 1.76–1.95 Å (Kamb 1972), giving an approximate area (πr^2) of 9.7–11.9 Å^2 around a central oxygen atom in the plane of the water molecule.

Table 3 Comparison of calculated and experimental elastic constants

	Elastic constants of Mg_2SiO_4/GPa								
	C_{11}	C_{22}	C_{33}	C_{44}	C_{55}	C_{66}	C_{12}	C_{13}	C_{23}
Exp.	329	200	236	67.2	81.4	81.1	66	68	73
Calc.	359	207	281	44.2	74.5	84.3	94	96	88

The initial sites chosen for molecular adsorption of water onto the surfaces were above surface oxygen ions and cations. When adsorbing onto the cation sites, the oxygen atom of the water molecule was initially positioned above the surface cation, after which the surface was allowed to relax and find the minimum energy configuration. Adsorption at the surface oxygen sites was modelled by positioning one of the water molecule's hydrogen atoms at a hydrogen-bond distance of 1.8 Å (Kamb 1972).

In the case of dissociative adsorption of water a dissociated water molecule was adsorbed on every surface magnesium-oxygen pair and, in effect, surface oxygen atoms were replaced by two hydroxyl groups, resulting in terminal MgOH and SiOH groups at the surface, i.e. in Kröger-Vink notation (Kröger 1964; van Gool 1966):

$$H_2O + O_o^x \rightarrow (OH)_o^\bullet + (OH)_i' \quad , \tag{5}$$

where O_o^x is an oxygen at a lattice oxygen site with zero charge with respect to the lattice oxygen, $(OH)_o^\bullet$ is a hydroxyl group at an oxygen lattice site with charge $+1$ and $(OH)_i'$ is a hydroxyl group at an interstitial site with charge -1. All charges are relative to the crystal lattice. In this study, we did not hydroxylate silicon-oxygen pairs, as the already four-coordinated silicon ion would then become five-coordinate, which, although not unknown in high-pressure studies, would be unlikely at a free surface.

Pure surfaces

We studied the low index surfaces of forsterite, including the {0 2 1} surface which is important in the experimental morphology (Deer et al. 1992). We considered both non-dipolar and dipolar terminations, and the surface energies of the unrelaxed and relaxed planes are listed in Table 4.

As is clear from its low relaxed surface energy, the non-dipolar termination of the {0 1 0} surface, which is the major cleavage plane of forsterite, is the most stable surface under dry conditions, in agreement with previous calculations (Watson et al. 1997). The relaxation energy of the non-dipolar {0 1 0}a surface is small and the relaxed surface energy of 1.28 J m^{-2} is very similar to that

Table 4 Unrelaxed and relaxed surface energies of unhydrated forsterite surfaces

Surface energies of unhydrated forsterite surfaces/J m^{-2}		
Surface[a]	Unrelaxed	Relaxed
{0 0 1}a[d]	3.84	1.74
{0 0 1}b[d]	7.22	2.30
{0 1 0}a	2.23	1.28
{0 1 0}b[d]	4.43	2.32
{1 0 0}a	8.50	2.57
{1 0 0}b[d]	4.60	2.25
{0 1 1}a	6.55	2.35
{0 1 1}b[d]	8.48	2.60
{1 0 1}a[d]	4.87	1.88
{1 0 1}b[d]	8.06	2.24
{1 1 0}a	9.15	3.18
{1 1 0}b[d]	3.55	1.96
{1 1 1}a[d]	5.45	2.29
{1 1 1}b[d]	4.00	1.81
{0 2 1}a[d]	4.67	1.94
{0 2 1}b[d]	7.49	2.38

[a] d denotes a dipolar plane

of the {0 0 1} surface of magnesium oxide (1.25 J m^{-2}; de Leeuw et al. 1995), whose structure it resembles. The {0 1 0} surface is a close-packed plane with a small surface area (28.6 $Å^2$ per unit cell) and cleaving the bulk crystal to create this surface does not involve the breaking of many bonds. As a result, the relaxed surface is almost bulk-terminated, showing only some flattening of the unrelaxed rumpled surface with the magnesium ions moving into the surface by some 0.3 Å.

Some of the more open-structured surfaces with larger surface areas per unit cell show much larger relaxations, such as the non-dipolar {0 1 1}a surface with a surface area of 56.7 $Å^2$ and the dipolar {0 2 1}b surface with a surface area of 75.3 $Å^2$. However, the largest surface relaxations take place when there are silica groups at the surface. For example, the non-dipolar {1 0 0} and {1 1 0} surfaces both have SiO_4 groups in the topmost layer and upon energy minimisation, the surface energies of both surfaces decrease by 6 J m^{-2}, the largest relaxations in the series. In both cases, the extensive surface relaxation involves rotation of the surface silica groups while magnesium ions from lower layers move up into the topmost layer. As a result, the immediate surface region assumes a more open structure. For example, Fig. 1 shows the unrelaxed and relaxed surface structure of the {1 0 0}a surface, which is one of the cleavage planes of forsterite, although not as common as the {0 1 0} surface. It shows the rotation of the silica tetrahedra and the formation of an almost stepped surface where the sides of the steps are terminated by magnesium ions, some of which have moved into the surface by 0.1–0.2 Å, while others have moved considerably out of the surface (1.24 Å).

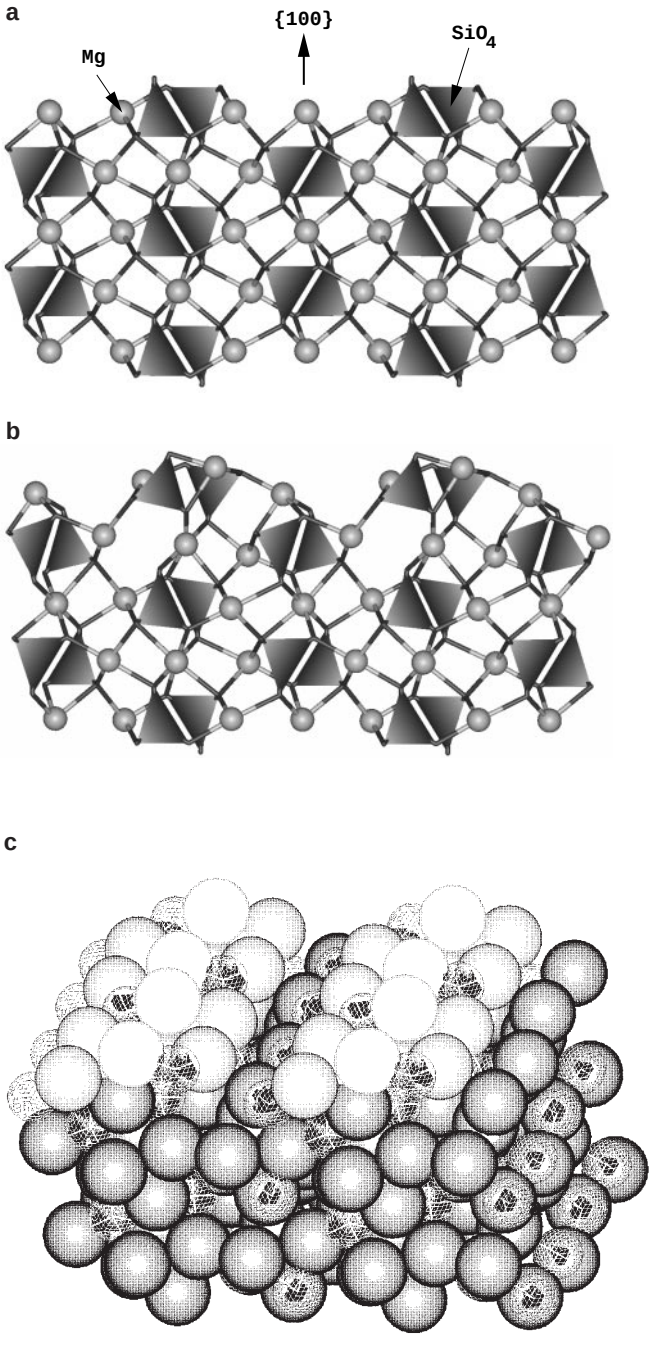

Fig. 1 Side view of the **a** unrelaxed and **b** relaxed surface structure of the non-dipolar {1 0 0} surface, showing rotation of surface silica groups and movement of magnesium ions into the topmost layer, and **c** three-dimensional view showing corrugation of the relaxed {1 0 0} surface with oxygen atoms shaded according to height from pale at the surface to dark in the bulk crystal (Mg shown as a mesh)

Associative adsorption

On associative adsorption of water and relaxation of the hydrated surfaces, all surfaces are stabilised with respect to the unhydrated surfaces, with adsorption energies ranging from 100–172 kJ mol^{-1} (Table 5). Fubini et al. (1989), in their temperature-programmed desorption (TPD) study of a variety of oxide surfaces, suggest that the associative adsorption of a water molecule by its oxygen atom to a surface metal ion releases energies of between 70 and 120 kJ mol^{-1}. Almost all water mole-

Table 5 Surface and adsorption energies of associative adsorption of water on relaxed forsterite surfaces

Surface[a]	γ/J m^{-2}	E_{ads}/kJ mol^{-1}
{0 0 1}a^{d}	0.47	−117.7
{0 0 1}b^{d}	1.36	−112.9
{0 1 0}a	0.30	−99.4
{0 1 0}b^{d}	0.86	−127.4
{1 0 0}a	1.37	−132.1
{1 0 0}b^{d}	1.28	−103.2
{0 1 1}a	0.28	−140.9
{0 1 1}b^{d}	0.96	−137.0
{1 0 1}a^{d}	1.02	−101.3
{1 0 1}b^{d}	1.14	−117.7
{1 1 0}a	1.29	−171.7
{1 1 0}b^{d}	0.35	−137.0
{1 1 1}a^{d}	1.01	−123.5
{1 1 1}b^{d}	0.79	−107.1
{0 2 1}a^{d}	0.60	−130.3
{0 2 1}b^{d}	1.50	−101.3

[a] d denotes a dipolar plane

cules also coordinate in a hydrogen-bonded fashion by their hydrogen atoms to oxygen ions either in the lattice or other water molecules. This type of interaction found in liquid water can be expected to release at least 44 kJ mol^{-1} or so and Fubini et al. (1989) estimate it to release another 50–70 kJ mol^{-1} when oxide surfaces are present. Hence, our calculated adsorption energies of 100–172 kJ mol^{-1}, which include both interactions, agree well with their findings.

The non-dipolar {0 1 0} surface remains one of the most stable surfaces although its hydration energy is the lowest. The less stable unhydrated surfaces show the largest adsorption energies and are stabilised most upon hydration. For example, the surface energy of the non-dipolar {1 1 0} surface, the most unstable dry surface, decreases from 3.18 J m^{-2} to 1.29 J m^{-2} when hydrated by molecular water and the process releases 171.7 kJ mol^{-1}. Figure 2 shows both the unhydrated and hydrated {1 1 0}a surfaces, from which it can be seen that some of the water molecules adsorb in the gaps on the surface, hence smoothing the surface. Another effect is that the water molecules cluster around magnesium ions and hence increase the coordination of the surface cations. In earlier work on surface hydration of different systems, namely MgO (de Leeuw et al. 1996), Al_2O_3 (de Leeuw and Parker 1999a) and calcium carbonates (de Leeuw and Parker 1998b), we also found large stabilisations of otherwise relatively unstable surfaces, which we suggest is a general effect.

Dissociative adsorption

The next step was to add dissociated water molecules onto the surfaces, in effect hydroxylating the topmost layer and again relaxing the surfaces. The surface and adsorption energies of the hydroxylated surfaces are collected in Table 6. Apart from the non-dipolar {1 0 0} surface, all surfaces are amenable to hydroxylation. On

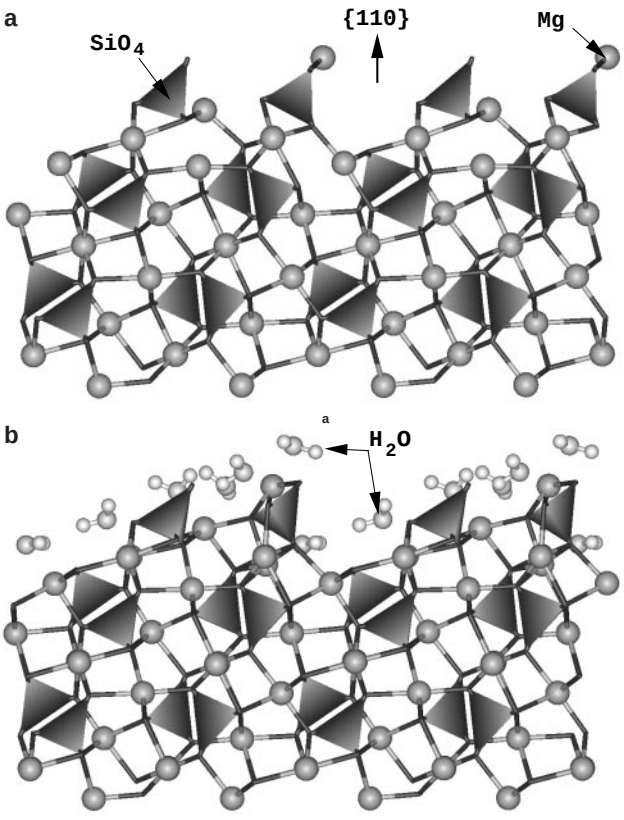

Fig. 2 a Relaxed unhydrated non-dipolar {1 1 0} surface and **b** minimum energy structure with water molecules associatively adsorbed in the surface gaps

some of the dipolar surfaces, notably the {0 1 0}, {0 1 1} and {1 1 1}a, large amounts of energy are released upon dissociative adsorption of water, but again, the largest adsorption energy is found for the non-dipolar {1 1 0} surface. Similarly to the {1 1 0} surface with associatively

Table 6 Surface and adsorption energies of dissociative adsorption of water on relaxed forsterite surfaces

Surface[a]	γ/J m^{-2}	E_{ads}/kJ mol^{-1}
{0 0 1}a^{d}	0.52	−120.6
{0 0 1}b^{d}	0.56	−256.7
{0 1 0}a	0.76	−89.2
{0 1 0}b^{d}	0.58	−300.1
{1 0 0}a	2.77	+73.3
{1 0 0}b^{d}	1.34	−168.8
{0 1 1}a	0.33	−172.7
{0 1 1}b^{d}	0.97	−278.8
{1 0 1}a^{d}	0.75	−178.5
{1 0 1}b^{d}	0.86	−217.1
{1 1 0}a	1.10	−420.7
{1 1 0}b^{d}	0.49	−150.5
{1 1 1}a^{d}	1.57	−316.8
{1 1 1}b^{d}	0.90	−152.4
{0 2 1}a^{d}	1.01	−141.8
{0 2 1}b^{d}	1.28	−167.9

[a] d denotes a dipolar plane

adsorbed water molecules, the hydroxylated {1 1 0} surface has been smoothed by adsorption of hydroxyl groups bridging the gaps on the surface and increasing the coordination of the surface magnesium ions.

Comparing the surface energies for the different surfaces in Tables 4–6 we see that on associative adsorption of water, all surface energies were reduced and the relative stabilities of the different cuts of each surface remain the same. However, on dissociative adsorption of water some of the surface energies have increased. Furthermore, the relative stability of different cuts can be modified: for example, the non-dipolar {0 1 0} surface was far more stable than the dipolar {0 1 0} plane both in the unhydrated form and after associative adsorption of water, but upon hydroxylation the dipolar cut has become more stable in a way similar to the dipolar and non-dipolar cuts of the α-Al_2O_3 {0 0 0 1} basal plane (Nygren et al. 1997; de Leeuw and Parker 1999a). The change in stability arises because the surface energy of the dipolar plane has decreased steadily from dry to associative adsorption to hydroxylation, but the surface energy of the non-dipolar {0 1 0} surface has increased from associative adsorption ($\gamma = 0.30$ J m^{-2}) to dissociative adsorption ($\gamma = 0.76$ J m^{-2}). In addition, the energy of adsorption of dissociated water molecules at -89 kJ mol^{-1} is less than for associative adsorption (-99 kJ mol^{-1}), and from both adsorption energies and surface energies we may assume that the non-dipolar {010} surface will be more stable when unhydroxylated. Figure 3 shows the unhydrated non-dipolar {0 1 0} surface and the hydroxylated dipolar {0 1 0} plane. The non-dipolar surface is a smooth plane terminated by O-Mg-O bridges. Hydroxylation of this plane leads to a much rougher surface. In a previous study on the stability of quartz surfaces (de Leeuw et al. 1999a), we found that the quartz {0 0 0 1} surface, which is terminated by O-Si-O bridges similar to the O-Mg-O bridges on the forsterite {0 1 0} surface, was not as amenable to dissociative adsorption of water as the other quartz surfaces, which have low-coordinated surface species. Furthermore, when we adsorbed concentrated NaOH on the quartz {1 0 1 1} surface we found that the formation of O-Na-O bridges had a large stabilising effect as well.

In contrast, hydroxylation of the dipolar {0 1 0} surface is energetically very favourable. The surface consists of a half-vacant magnesium plane. The hydroxyl groups of the dissociated water molecules strongly bond to two surface magnesium ions (Fig. 3b). Their hydrogen atoms, together with the hydrogens bonded to lattice oxygens, tilt towards the magnesium vacancies. This is a structural analogue of the hydrogarnet defect in grossular (Wright et al. 1994), where four hydrogen atoms are found to point in the direction of an empty silicon site. We observed the same effect on hydroxylation of a stepped MgO {1 0 0} surface, where again the hydrogen atoms of adsorbed hydroxyl groups pointed towards empty Mg lattice sites (de Leeuw et al. 1995) and on dissolution of Mg ions from corner sites (de Leeuw and Parker 1999a).

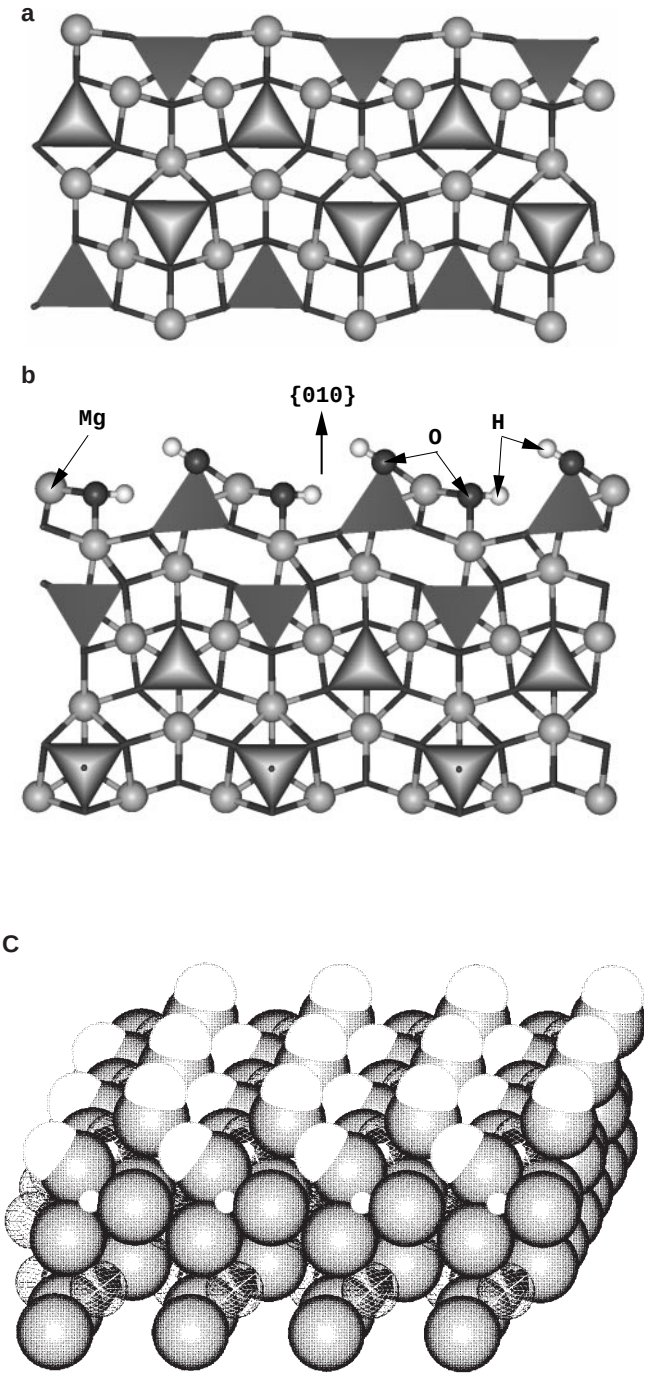

Fig. 3 **a** Side view of the relaxed unhydrated non-dipolar {0 1 0} surface showing a smooth plane of O-Mg-O bridges. **b** Side view of the hydroxylated dipolar {010} surface showing extensive coordination between surface Mg ions and hydroxyl groups. **c** Three-dimensional view of the hydroxylated dipolar {0 1 0} surface showing corrugation of the surface with rows of hydroxy groups at different heights (Mg shown in mesh)

Next, we adsorbed a layer of water molecules on each hydroxylated surface and the resulting surface and adsorption energies are collected in Table 7. Almost all surfaces have been stabilised with low adsorption energies indicative of physisorption of the water mole-

cules to the hydroxylated surfaces. Fubini et al. (1989), in their TPD study of a range of hydrated oxides, found energies of between 50 and 70 kJ mol^{-1} for adsorption of water molecules to hydrogen atoms of surface hydroxyl groups. On the surfaces where the adsorption is much larger, notably the {1 1 0}a, {1 1 1}a and {0 2 1}b surfaces, we find that some of the water molecules also coordinate to surface magnesium and silicon ions. The stabilities of the two {0 1 0} planes are still reversed, with the dipolar plane the more stable of the two, although the difference in surface energies (0.1 J m^{-1}) is small enough that we may expect, at the macroscopic scale, to find a stepped surface containing both planes under aqueous conditions.

Magnesium dissolution

The greater stability of the hydroxylated dipolar {0 1 0} plane over the non-dipolar plane suggests that some dissolution of the magnesium ions may occur upon hydration, as is, for example, observed experimentally for wollastonite ($CaSiO_3$) (KH Rao, personal communication) and can be induced for forsterite at low pH. Seyama et al. (1996), for example, used X-ray photoelectron spectroscopy to investigate removal of magnesium ions from forsterite surfaces. After acid dissolution they only found surface $SiO_2{\cdot}nH_2O$ species, while micrographs showed an etched structure. In addition, high-temperature vacuum experiments by Nagahara and Ozawa (1996) and Young et al. (1998) showed forsterite to evaporate in H_2 gas, leaving pits and islands on the surface. We calculated dissolution of surface magnesium ions to be energetically feasible for a range of MgO surfaces of differing cation coordination (de Leeuw and Parker 1999a) and we were interested to see whether the same was true for both the dipolar and non-dipolar forsterite {010} surfaces. To this end we replaced surface magnesium ions by two hydrogen ions each, in effect dissolving a Mg^{2+} ions under acidic conditions. Thus, to calculate the dissolution energy we investigate the following reaction:

$$2H^{+}_{(aq)} + \text{Surface}_{\text{pure}} \rightarrow \text{Surface}_{\text{defective}} + Mg^{2+}_{(aq)} \quad , \qquad (6)$$

where experimental enthalpies for $H^{+}_{(aq)}$, $Mg^{2+}_{(aq)}$ and water and the simulated results for $\text{Surface}_{\text{pure}}$ and $\text{Surface}_{\text{defective}}$ were used.

The dissolution energy, i.e. the energy of replacing a magnesium ion by two hydrogen ions, for the non-dipolar plane was −204.4 kJ mol^{-1} while the dissolution energy for the dipolar plane was −381.5 kJ mol^{-1}, clearly a more favourable process. Thus, we find that dissolution of magnesium ions from both surfaces is energetically favourable under acidic conditions, providing a route for obtaining the most stable surface under different conditions. The surfaces, including defects, were then hydrated by molecular water again, which released another 63.1 and 130.9 kJ mol^{-1} for the non-dipolar and dipolar surfaces respectively which is similar to the energy released on adsorbing water to the hydroxylated non-dipolar surface, 71.4 kJ mol^{-1} (see Table 7) but larger than for the dipolar surface, 67.5 kJ mol^{-1}.

Table 7 Surface and adsorption energies of associative adsorption of water on relaxed hydroxylated forsterite surfaces

Surface[a]	γ/J m^{-2}	E_{ads}/kJ mol^{-1}
{0 0 1}a^{d}	0.08	−68.5
{0 0 1}b^{d}	0.28	−64.6
{0 1 0}a	0.27	−71.4
{0 1 0}b^{d}	0.17	−67.5
{1 0 0}a	–	–
{1 0 0}b^{d}	0.78	−78.2
{0 1 1}a	0.16	−55.0
{0 1 1}b^{d}	0.55	−72.4
{1 0 1}a^{d}	0.91	−32.8
{1 0 1}b^{d}	0.32	−80.1
{1 1 0}a	0.26	−102.3
{1 1 0}b^{d}	0.20	−63.7
{1 1 1}a^{d}	1.81	−126.4
{1 1 1}b^{d}	0.84	−48.2
{0 2 1}a^{d}	0.28	−90.7
{0 2 1}b^{d}	0.32	−105.2

[a] d denotes a dipolar plane

Morphology

The equilibrium morphology of a crystal is determined by the surface energy and the related growth rate of the various surfaces and provides a measure of the relative stabilities of the surfaces. Wulff's Theorem (Wulff 1901) proposed that a polar plot of surface energy versus orientation of normal vectors would give the crystal morphology based on the approach of Gibbs (Gibbs 1928), who proposed that under thermodynamic control the equilibrium form of a crystal should possess minimal total surface free energy for a given volume. We consider that for solid surfaces the surface energy is a close approximation for the surface free energy because previous lattice dynamics simulations showed that the contribution of the excess entropy term to the surface free energy is small compared to the enthalpy term, as the differences between the entropies of the bulk and the surface are small. Thus, the surface energies can be assumed to determine the equilibrium morphology of the crystal. Moreover, we would expect a surface with a high surface free energy to have a large growth rate and this fast-growing surface will not be expressed in the morphology of the resulting crystal. Only surfaces with low surface free energies, and hence slow-growing, will be expressed. However, crystal growth is a complex kinetic process and will be affected by many factors and hence the equilibrium morphologies should be treated more as a representation of the effect of the addition of water to the different surfaces rather than the definitive growth morphology.

Figure 4a shows a common experimental morphology expressing surfaces investigated in this paper

(Deer et al. 1992). From the surface energies of the hydrated and hydroxylated surfaces we calculated an equilibrium morphology for forsterite (Fig. 4b). The surfaces for which the energy of dissociative adsorption was equal or less than that of associative adsorption were deemed not to become hydroxylated. There is a good comparison between the morphology thus obtained with the experimental morphology: the same surfaces are expressed in the calculated equilibrium morphology as are found in the experimental morphology, although both {0 0 1} and {1 1 0} surfaces are somewhat too stable with respect to the {1 0 1} and {0 2 1} planes.

Conclusion

This study has advanced considerably our understanding of the surface stability and structure of forsterite. We have shown first that on energy minimisation of the unhydrated surfaces large relaxations of the silica terminated planes occur, with magnesium ions moving into the surface layer and a general smoothing of the surfaces. The non-dipolar {0 1 0} plane is the most stable forsterite surface in unhydrated form and its stability may be due to the formation of O-Mg-O bridges on the surface, similar to O-Si-O and O-Na-O bridges, which were found to stabilise surfaces of α-quartz.

Next we have shown that all surfaces are amenable to associative adsorption of water with adsorption energies ranging from 100–170 kJ mol^{-1}, indicative of chemisorption of the oxygen of the water molecule to metal cations in the surface combined with hydrogen bonding to lattice oxygen ions and other water molecules. We have shown that dissociative adsorption is energetically favourable on most surfaces. On the surfaces where associative adsorption leads to hydroxylation, the adsorption energies exceed 120 kJ mol^{-1}, in agreement with experimental findings by Fubini et al. (1989) in their TPD study of a variety of oxide surfaces.

An important finding is that dissolution of Mg^{2+} ions with replacement by H^{+} ions is energetically feasible on both {0 1 0} terminations, showing that the reversed stability of the two planes from associative to dissociative water adsorption need not impede the occurrence of the more stable dipolar plane under aqueous conditions.

We also found that the equilibrium morphology obtained using the surface energies of the various hydrated surfaces agrees well with the experimentally found morphology, indicating that the relative stabilities of the surfaces were modelled correctly.

Future work will apply molecular dynamics simulations to the various surfaces in liquid water to allow temperature to be included in the calculations. Furthermore, we intend in future to use the same static simulation techniques to study the relative stabilities of forsterite grain boundaries and hydration effects therein, in addition to molecular dynamics simulations of diffusion along the grain boundaries.

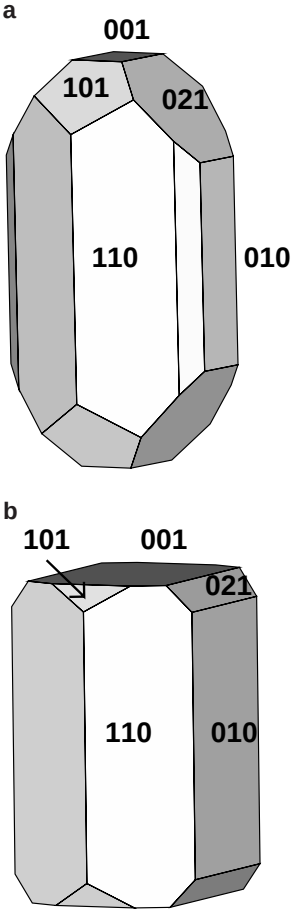

Fig. 4 **a** Experimental and **b** calculated equilibrium morphology of forsterite

Acknowledgements We thank NERC, (grant no. GR3/11779) for financial support and Molecular Simulations Inc. for the use of InsightII. We wish to acknowledge the use of the EPSRC's Chemical Database Service at Daresbury.

References

Baram PS, Parker SC (1996) Atomistic simulation of hydroxide ions in inorganic solids. Philos Mag B 73:49–58

Born M, Huang K (1954) Dynamical theory of crystal lattices. Oxford University Press, Oxford

Catlow CRA, Price GD (1990) Computer modeling of solid-state inorganic materials. Nature 347:243–248

Chang F-RC, Skipper NG, Sposito G (1995) Computer simulation of interlayer molecular structure in sodium monmorillonite hydrates. Langmuir 11:2734–2741

Dana ES (1941) A textbook of mineralogy. John Wiley, New York

Davies MJ (1992) PhD Thesis, University of Bath, UK

Deer WA, Howie RA, Zussman J (1992) Introduction to the rock-forming minerals. Longman, Harlow, UK

de Leeuw NH, Parker SC (1997) Atomistic simulation of the effect of molecular adsorption of water on the surface structure and energies of calcite surfaces. J Chem Soc Faraday Trans 93:467–475

de Leeuw NH, Parker SC (1998a) Molecular dynamics simulation of MgO surfaces in liquid water using a shell model potential for water. Phys Rev B58:13901–13908

de Leeuw NH, Parker SC (1998b) Surface structure and morphology of calcium carbonate polymorphs calcite, aragonite and vaterite: an atomistic approach. J Phys Chem B102:2914–2922

de Leeuw NH, Parker SC (1999a) Computer simulation of dissociative adsorption of water on CaO and MgO surfaces and the relation to dissolution. Res Chem Intermed 25:195–211

de Leeuw NH, Parker SC (1999b) The effect of chemi- and physisorption of water on the surface structure and stability of α-alumina. J Am Ceram Soc 82:3209–3216

de Leeuw NH, Watson GW, Parker SC (1995) Atomistic simulation of the effect of dissociative adsorption of water on the surface structure and stability of calcium and magnesium oxide. J Phys Chem 99:17219–17225

de Leeuw NH, Watson GW, Parker SC (1996) Atomistic simulation of adsorption of water on three-, four- and five-coordinated surface sites of magnesium oxide. J Chem Soc Faraday Trans 92:2081–2091

de Leeuw NH, Higgins FM, Parker SC (1999a) Modelling the surface structure and stability of a-quartz. J Phys Chem B103:1270–1277

de Leeuw NH, Parker SC, Harding JH (1999b) Molecular dynamics simulation of crystal dissolution from calcite steps. Phys Rev B 60:13792–13799

Dick BG, Overhauser AW (1958) Theory of the dielectric constants of alkali halide crystals. Phys Rev 112:90–103

Duan Z, Moller N, Weare JH (1995) Molecular dynamics simulation of water properties using RWK2 potential: from clusters to bulk water. Geochim Cosmochim Acta 59:3273–3283

Dubrovinskaya NA, Dubrovinsky LS, Saxena SK (1997) Systematics of thermodynamic data on solids: thermochemical and pressure-volume-temperature properties of some minerals. Geochim Cosmochim Acta 61:4151–4158

Fubini B, Bolis V, Bailes M, Stone FS (1989) The reactivity of oxides with water vapor. Solid State Ionics 32:258–272

Gibbs JW (1928) Collected works. Longman, New York

Greenberg SA (1957) Thermodynamic functions for the solution of silica in water. J Phys Chem 61:196–197

Harding JH, Pyper NC (1995) The meaning of the oxygen 2nd electron affinity and oxide potential models. Philos Mag Lett 71:113–121

Hirth G, Kohlstedt DL (1995) Experimental constraints on the dynamics of the partially molten upper-mantle .2 Deformation in the diffusion creep regime (1995). J Geophys Res Solid Earth 100:1981–2001

Iishi K (1978) Lattice dynamics of forsterite. Am Mineral 63:1198–1208

Iler RK (1979) The chemistry of silica; solubility polymerisation, colloid and surface properties, and biochemistry. John Wiley, New York

Kamb B (1972) Water and aqueous solutions. Horne RA (ed) John Wiley, New York

Kerschhofer L, Sharp TG, Rubie DC (1996) Intracrystalline transformation of olivine to wadsleyite and ringwoodite under subduction zone conditions. Science 274:79–81

Kohlstedt DL, Zimmerman ME (1996) Rheology of partially molten mantle rocks. Annu Rev Earth Plan Sci 24:41–62

Kohn SC (1996) Solubility of H_2O in nominally anhydrous mantle minerals using H-1 MAS NMR. Am Mineral 81:1523–1526

Kröger FA (1964) The chemistry of imperfect crystals. North Holland Press, Amsterdam

Lewis GV, Catlow CRA (1985) Potential models for ionic oxides. J Phys C. Solid State Phys 18:1149–1161

Mitchell MBD, Jackson D, James PF (1998) Preparation and characterisation of forsterite (Mg_2SiO_4) aerogels. J Non-Cryst Solids 225:125–129

Nagahara H, Ozawa K (1996) Evaporation of forsterite in H_2 gas. Geochim Cosmochim Acta 60:1445–1459

Nygren MA, Gay DH, Catlow CRA (1997) Hydroxylation of the surface of the corundum basal plane. Surf Sci 380:113–123

Parker SC, Price GD (1989) Computer modelling of phase transitions in minerals. Adv Solid State Chem 1:295–327

Parry DE (1975) The electrostatic potential in the surface region of an ionic crystal. Surf Sci 49:433–440

Parry DE (1976) Errata. Surf Sci 54:195

Price GD, Parker SC, Leslie M (1987) The lattice dynamics of forsterite. Mineral Mag 51:157–170

Purton JA, Allan NL, Blundy JD (1997) Calculated solution energies of heterovalent cations in forsterite and diopside: implications for trace element partitioning. Geochim Cosmochim Acta 61:3927–3936

Purton JA, Allan NL, Blundy JD, Wasserman EA (1996) Isovalent trace element partitioning between minerals and melts: a computer simulation study. Geochim Cosmochim Acta 60:4977–4987

Sanders MJ, Leslie M, Catlow CRA (1984) Interatomic potentials for SiO_2. J Chem Soc Chem Commun 1271–1273

Saul P, Catlow CRA, Kendrick J (1985) Theoretical studies of protons in sodium hydroxide. Phil Mag B51:107–117

Schroder KP, Sauer J, Leslie M, Catlow CRA, Thomas JM (1992) Bridging hydroxyl-groups in zeolitic catalysts – a computer simulation of their structure, vibrational properties and acidity in protonated faujasites (H-Y zeolites). Chem Phys Lett 188:320–325

Seyama H, Soma M, Tanaka A (1996) Surface characterisation of acid-leached olivines by X-ray photoelectron spectroscopy. Chem Geol 129:209–216

Smyth JR, Hazen RM (1973) Crystal structures of forsterite and hoirtolonite at several temperatures up to 900 degrees C. Am Mineral 58:588–593

Tasker PW (1979) The surface energies, surface tensions and surface structure of the alkali halide crystals. Phil Mag A39:119–136

van Gool W (1966) Principles of defect chemistry of crystalline solids. Academic Press, New York

Watson GW, Kelsey ET, de Leeuw NH, Harris DJ, Parker SC (1996) Atomistic simulation of dislocations, surfaces and interfaces in MgO. J Chem Soc Faraday Trans 92:433–438

Watson GW, Oliver PM, Parker SC (1997) Computer simulation of the structure and stability of forsterite surfaces. Phys Chem Miner 25:70–78

Weast RC, Astle MJ (1981) CRC Handbook of chemistry and physics, CRC Boca Raton

Wieland E, Wehrli B, Stumm W (1988) The coordination chemistry of weathering: III. A generalization on the dissolution rates of minerals. Geochim Cosmochim Acta 52:1969–1981

Wright K, Catlow CRA (1994) A computer-simulation study of (OH) defects in olivine. Phys Chem Miner 20:515–518

Wright K, Freer R, Catlow CRA (1994) The energetics and structure of the hydro-garnet defect in grossular – a computer-simulation study. Phys Chem Miner 20:500–503

Wulff G (1901) Zur Frage der Geschwindigheit des Wachstums und der Auflösung der Krystallflachen. Z Kristallogr Kristallgeom 34:949

Young ED, Nagahara H, Mysen BO, Audet DM (1998) Non-Rayleigh oxygen isotope fractionation by mineral evaporation: theory and experiments in the system SiO_2. Geochim Cosmochim Acta 62:3109–3116